Journal of ELECTRONIC MATERIALS, Vol. 45, No. 6, 2016
DOI: 10.1007/s11664-016-4364-1

Direct-Coated Photoconducting Nanocrystalline PbS Thin Films with Tunable Band Gap

DHAVAL VANKHADE,[1] ANJANA KOTHARI,[1] and TAPAS K. CHAUDHURI[1,2]

1.—Dr. K. C. Patel Research and Development Centre, Charotar University of Science and Technology, Anand District, Gujarat, Changa 388421, India. 2.—e-mail: tkchaudhuri.rnd@charusat.ac.in

Nanocrystalline PbS thin films are deposited on glass by direct coating from a precursor solution of lead acetate and thiourea in methanol. A single coating has a thickness of 50 nm and greater thicknesses are obtained from layer by layer deposition. The films are smooth and shiny with roughness (rms) of about 1.5 nm. X-ray diffraction studies show that films are cubic PbS with crystallite size about 10 nm. The films are *p*-type with dark electrical conductivities in the range of 0.4–0.5 S/cm. These films are basically photoconducting. Photoconductivity monotonically increases with increase in thickness. The band gap of the films strongly depends on the thickness of the films. The band gap decreases from 2.4 eV to 1.6 eV as the thickness is increased from 50 nm to 450 nm. The tunability of the band gap is useful for technical applications, such as solar cells and photodetectors.

Key words: Lead sulfide, thin films, nanocrystalline, tunable band gap, photoconducting

INTRODUCTION

Films of nano-sized lead sulfide (PbS) has emerging as an extraordinary material for photovoltaics[1–16] and photodetectors[17–23] because of a significant size-dependent and tunable band gap.[24–26] Basically, normal bulk PbS is a IV–VI earth-abundant semiconductor with a narrow direct band gap of 0.41 eV at 300 K and absorption coefficient greater than 10^4 cm^{-1}. These photoconducting PbS films are used as near-infrared detectors with sensitivity in the wavelength range of 1–3 μm. PbS also has a large excitonic Bohr radius of 18 nm because of high dielectric constant 17.2 and low effective mass of electrons. Hence, it exhibits a strong quantum size effect for larger quantum dots (QDs) (<18 nm) as compared to CdS or CdSe. Thus, the band gap of PbS QDs can be easily tuned from 0.41 (bulk) to 4 eV by selecting appropriate size.

PbS QDs synthesized by a hot-injection method using two distinct chemical routes.[27,28] The first method, described by Hines and Scholes,[27] is based on the reaction of lead oleate with bis(trimethylsilyl)-sulfide in octadecene which yields monodispersed QDs of sizes ranging from 2.6 nm to 7.2 nm. These QDs are bright but not fully air-stable. The second procedure suggested by Cademartiri et al.[28] utilizes the reaction between lead chloride and elemental sulfur in oleylamine as a solvent, producing QDs of sizes 4.2 nm and 6.4 nm. These QDs have a high PL quantum yield and thin films show good optical stability.

The fabrication of PbS QD devices as mentioned above is imperative to make thin films. PbS QD films are generally deposited by spin[15] or spray[29] from a suspension of QDs solvent. Before deposition of films, the QDs undergo several processing steps, such as controlled chemical synthesis with a capping agent, separation, removal of capping by ligand exchange and finally suspension in an appropriate solvent. These multi-steps not only render the QD film fabrication technique rather complex but also time consuming. Alternatively, a simple one-step deposition of nanoscale PbS thin films is desirable since it will simplify the fabrication of the devices.

(Received September 23, 2015; accepted January 19, 2016; published online February 19, 2016)

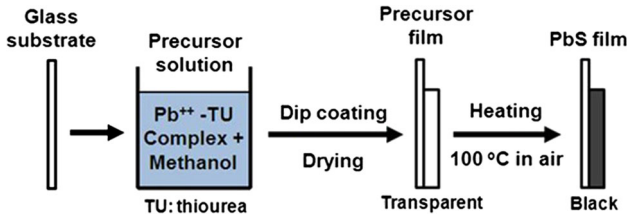

Fig. 1. Direct coating of PbS films on glass from a precursor solution.

Nanocrystalline PbS films can be deposited by chemical bath deposition (CBD) methods,[30–34] but these methods are cumbersome in thickness and particle size and also have a low material usage factor. However, examination of a direct coating method reported by Chaudhuri et al.[35] revealed that films dip-coated from a methanolic solution of lead acetate (LA) and thiourea (TU) complex yielded nanocrystalline PbS films. In this paper, we report the preparation and characterization of nanocrystalline PbS films along with preliminary electrical properties in the dark and light. Further, the band gap of these films can be tuned from 1.6 eV to 2.4 eV by varying the thickness.

EXPERIMENTAL

Deposition of PbS Film

PbS films were deposited on glass substrates by a direct liquid coating from a precursor solution of a LA-TU complex as described earlier by Chaudhuri et al.[35] and shown in Fig. 1. The precursor solution was prepared by dissolving LA (0.05 mol/L) and TU (0.05 mol/L) in methanol. Scrupulously cleaned glass substrates ($7.5 \times 2.5 \times 0.2$ cm^3) were first dip-coated with precursor films from the solution and dried at ~70°C in an oven. The transparent precursor layers heated at 100°C in air for 10 min resulted in shiny brown-black films of PbS having a thickness of about 50 nm. Greater thicknesses of PbS films were obtained by layer-by-layer deposition (LBL). The chemicals used were of analytical grade supplied by Merck, India.

The thicknesses of the films were measured by a surface profiler (Dektak 150, Veeco). Since dip-coating leads to some variation in thickness, the average was found by measuring thicknesses at 5 different places along the length of the film. The reported film thicknesses are accurate within ±10 nm for 50 and 100 nm and ±5 nm for thicknesses above 100 nm.

Characterization

The composition and crystalline status of the films was determined from x-ray diffraction (XRD) using a Bruker D2 Phaser Diffractometer in the 2θ range of 20° to 60°. Surface morphology of the films was examined by atomic force microscopy (AFM) using Nanosurf EasyScan2. Optical properties of thin films were examined by spectrophotometer (Shimadzu 3600) in the wavelength range 350 nm to 2400 nm. For electrical measurements, gap cells (10 mm × 5 mm) were made with colloidal graphite (Ted Pella) as ohmic contacts. The current was measured with a Source/Meter Unit (Keithley 2611) by applying 20 V/cm between the graphite electrodes. Photoconductivity of the films was measured by illuminating the samples with 80 mW/cm^2 light from halogen lamp (50 W, 12 V; Philips). To determine the type of conduction, the thermoelectric power (TEP) was also measured.

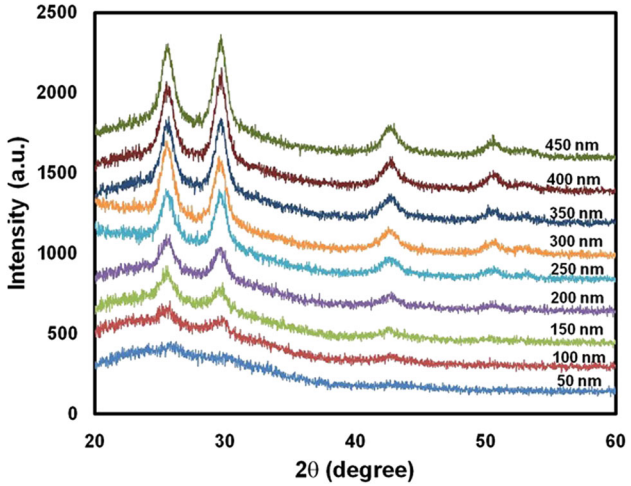

Fig. 2. X-ray diffraction plots of nanocrystalline PbS films on glass.

RESULTS AND DISCUSSION

Composition and Morphology

Heat treatment (100°C in air for 10 min) of transparent precursor films resulted in shiny black-brown films. XRD studies revealed that these films are crystalline with the cubic structure of PbS. That is, films containing the Pb^{+2}-TU complex thermally decomposed into PbS. Figure 2 presents the XRD plots of the PbS films deposited by LBL on glass substrates with thicknesses ranging from 50 nm to 450 nm. XRD plots show four broad diffraction lines with a background hump due to the glass substrate. The XRD lines are at 25.52°, 29.62°, 42.59° and 50.60°, which were identified due to reflections from (111), (200), (220) and (311) planes, respectively, of standard cubic PbS (JCPDS:05-592). That is, the films are pure cubic PbS without any other phases. Broad XRD lines (FWHM ~ 1°) indicate that the films are essentially nanocrystalline. The crystallite size estimated from broadening of the (111) and (200) lines using the Scherrer relationship[36] is 10 nm irrespective of thickness.

The surface morphology of a typical PbS film as observed by AFM shown in Fig. 3. The films are smooth with a root-mean-square roughness of

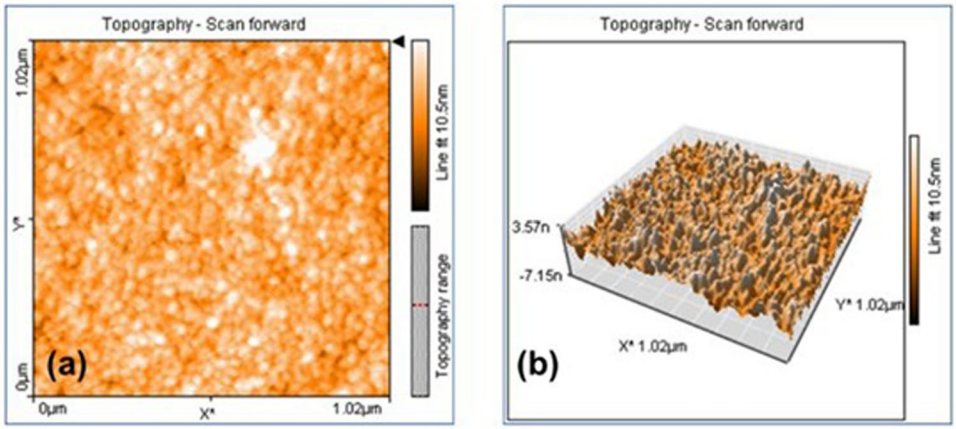

Fig. 3. Atomic force microscope image of a typical nanocrystalline PbS film (250 nm) on glass (a) 2 dimensional and (b) 3 dimensional.

1.5 nm. The film consists of spherical grains of 10 nm diameter.

Optical Properties

The transmission spectra of PbS films of different thicknesses in the wavelength range 350–2400 nm are shown in Fig. 4. As mentioned above, the films were deposited layer-by-layer and the thicknesses varied from 50 nm to 450 nm. The transmission spectrum of each film has two regions: an absorbing region at lower wavelengths and a non-absorbing region at higher wavelengths. In the absorbing region, the transmittance of a particular film rapidly diminishes below a certain wavelength corresponding to the absorption edge (where $h\nu \geq E_g$) and this wavelength decreases as the thickness decreases. In the non-absorbing region (where $h\nu \leq E_g$), the transmittance decreases or increases due to the presence of interference patterns because of multiple reflections of glass and film. The band gap (E_g) of nanocrystalline PbS films of different thicknesses (50–450 nm) is deduced from the Tauc relationship[37] for direct band gap semiconductors. The absorption coefficient (α) at each wavelength is calculated from the transmittance spectra.[38] The Tauc plots of $(\alpha h\nu)^2$ versus $h\nu$ for PbS films of different thicknesses are shown in Fig. 5. The E_g of the films determined from individual Tauc plots vary from 1.6 eV to 2.4 eV. Figure 6 presents the variation of E_g of nanocrystalline PbS films with thickness. The E_g of the films gradually decrease from 2.4 eV to 1.6 eV as the thickness increases from 50 nm to 450 nm, and this figure also indicates that the band gap of these PbS films is strongly dependent on thickness. That is, these nanocrystalline PbS films have tunable band gaps just like PbS QDs, only the controlling factor is thickness. The lower the thickness of the film, the larger the band gap. This property makes these nanocrystalline PbS films suitable for technical applications. Nanocrystalline PbS films can be envisaged as a 2-dimensional array of PbS nanoparticles or QDs with a narrow dispersion in size. The band gap of nanocrystalline PbS films depend on the dominant size of the nanoparticles that constitute the film. Hence, the size of the nanoparticles that comprises a film can be estimated from the E_g. The correlation between the size of the PbS nanoparticles (d) and the band gap (E_g) is given by the relationship of Moreels et al.[26] Table I presents the thickness of the PbS films, the optical band gap and the corresponding size of PbS QDs nanoparticles, revealing that the size of the PbS nanoparticles increases as the thickness of the PbS film increases. The sizes vary from 1.52 nm (50 nm) to 2.36 nm (500 nm). The increment in particle size is marginal. In the present study, PbS films are deposited layer-by-layer and each layer has a thickness of about 50 nm. The precursor film is deposited first and then heated at 100°C for 10 min in air to thermo-chemically convert the precursor to PbS. This means that every time a PbS film is deposited on top of another, the whole stack of films undergo thermal treatment at 100°C for 10 min. The marginal increase in the size of PbS nanoparticles in films is due to the annealing effect which imparts tunability of the band gap through thickness. The tunability of the band gap has been previously observed by several authors[30–34] for CBD nanocrystalline PbS films by regulating the process parameters. However, the band gap tunability of PbS films via thickness has not been reported by any of these authors.

Electrical and Photoconducting

The as-deposited nanocrystalline PbS films were p-type and photoconducting.

The photoconductivity (σ_{PH}) of a film under steady illumination is given by,

$$\sigma_{PH} = \sigma_D - \sigma_L \quad (1)$$

where σ_D is the conductivity in dark and σ_L the conductivity in light.

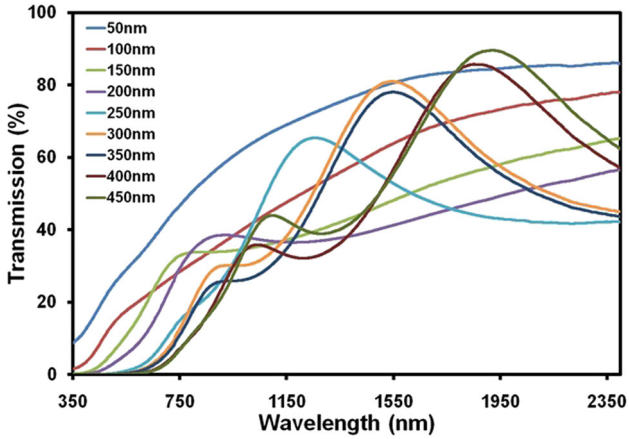

Fig. 4. Transmission spectra of nanocrystalline PbS films on glass.

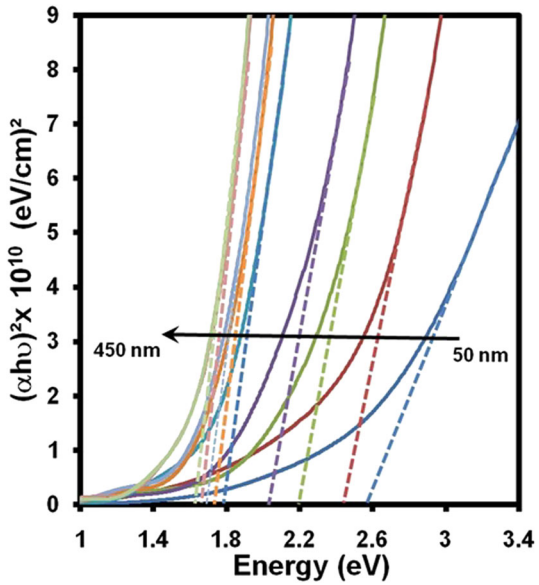

Fig. 5. Tauc plots for nanocrystalline PbS films on glass for determining the band gaps.

The photosensitivity (S) of the film is then written as

$$S = \sigma_{PH}/\sigma_D \quad (2)$$

Photoconductivity can be also expressed in terms of photogeneration, recombination time and mobility:

$$\sigma_{PH} = eG\tau\mu \quad (3)$$

where e is the charge of an electron, G is the generation rate of photocarriers (cm^{-3}), τ is the recombination time (s), and μ is the photocarriers mobility (cm^2/V s).

For a semitransparent PbS film of thickness d, the generation rate (G) of photocarriers is given by

$$G = \eta I_0(1-R)[1-\exp(-\alpha d)] \quad (4)$$

where η is the quantum efficiency of the generation of photocarriers, I_0 is the incident photon flux having energy greater than the band gap (photons/cm^2 s), R is the reflectivity of the film, and α is the absorption coefficient (cm^{-1}).

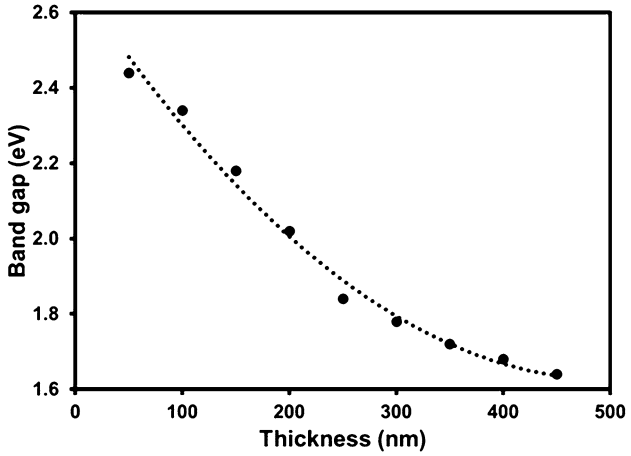

Fig. 6. Variation of band gaps of nanocrystalline PbS films with their thicknesses.

In Eq. 4, the $(1 - R)$ term indicates the fraction of incident light entering the film after reflection at the surface and the $[1 - \exp(-\alpha d)]$ term denotes the fraction of light absorbed in the film.

Hence, photoconductivity can be written as

$$\sigma_{PH} = e\eta I_0(1-R)[1-\exp(-\alpha d)]\tau\mu \quad (5)$$

Then, photosensitivity is also expressed as

$$S = e\eta I_0(1-R)[1-\exp(-\alpha d)]\tau\mu/\sigma_D \quad (6)$$

The variation of electrical conductivity of PbS films in the dark (σ_D) and under light (σ_L) is shown in Fig. 7. The dark conductivities of the films increase slowly and linearly with thickness. Thus, σ_D increases from 0.38 S/cm to 0.53 S/cm as the thickness increases from 50 nm to 450 nm. However, σ_L increases rapidly with thickness as shown in Fig. 7. The conductivities in light increase from 0.87 S/cm to 2.04 S/cm as the film thickness increases from 50 nm to 450 nm. Hence, the photoconductivities (σ_{PH}) of PbS films also increase rapidly and non-linearly as the thickness of films increases. The variation of the photosensitivity (S) of PbS films with thickness is depicted in Fig. 8. The photosensitivity increases from 1.38 to 2.87 as the thickness of the films varies from 50 nm to 450 nm.

Dark conductivity of PbS films did not change much with thickness: from about 0.4 S/cm for 50 nm to about 0.5 S/cm for 450 nm (Fig. 7). This is because nanocrystalline PbS films were deposited layer-by-layer and each layer of 50 nm deposited is independent of the other layers underneath. The small variation in σ_D may be due to the annealing and oxidation effect since each layer of PbS is thermolysed at 100°C in air for 10 min. However, the variation of photoconductivity of the PbS films with thickness is rapid (Fig. 7): 0.5 S/cm for 50 nm to 1.5 S/cm for 450 nm. This trend can be explained

Table I. Variation of nanoparticle size as a function of thickness of PbS films

Thickness (nm)	Optical band gap (eV)	Estimated nanoparticle size (nm)[26]
50	2.44	1.52
100	2.34	1.61
150	2.18	1.72
200	2.02	1.88
250	1.84	2.09
300	1.78	2.16
350	1.72	2.23
400	1.68	2.31
450	1.64	2.36
500	1.62	2.41

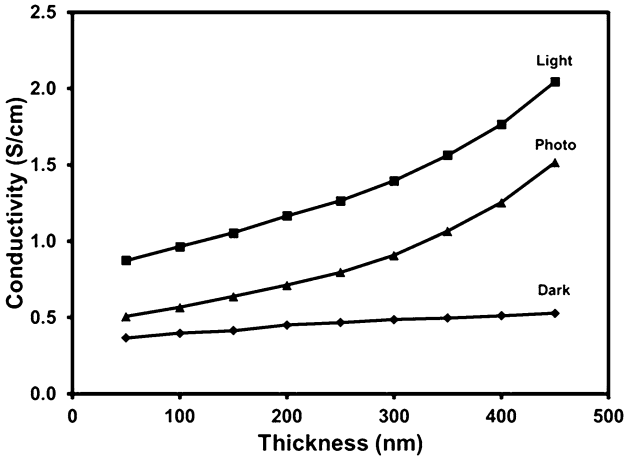

Fig. 7. Electrical conductivity of nanocrystalline PbS films in the dark and under illumination for different thicknesses.

on the basis of Eq. 5, because if it is assumed that all the films are illuminated by a light having the same photon flux (I_0) with energies more than the band gap ($h\nu \geq E_g$), then according to Eq. 5 photoconductivity (σ_{PH}) depends on how many photons are actually absorbed by the film. The absorption of photons for a film of thickness d is expressed as $[1 - \exp(-\alpha d)]$. As the thickness increases, the absorption of the photons increases non-linearly and hence the photoconductivity (Eq. 3) also increases. However, since the band gap of each film is different, there may be some deviation in the incident photon flux (I_0). Further, it is assumed that the reflectance (R) of different films is the same and that there are no interference effects, but actually interference does occur at these thicknesses. In spite of all these variations in the incident photon flux, the trend of non-linear increase in photoconductivity with the thickness of PbS films will be observed. Reports[33,34] on electrical properties of nanocrystalline PbS are very few. Hussain et al.[34] found that nanocrystalline

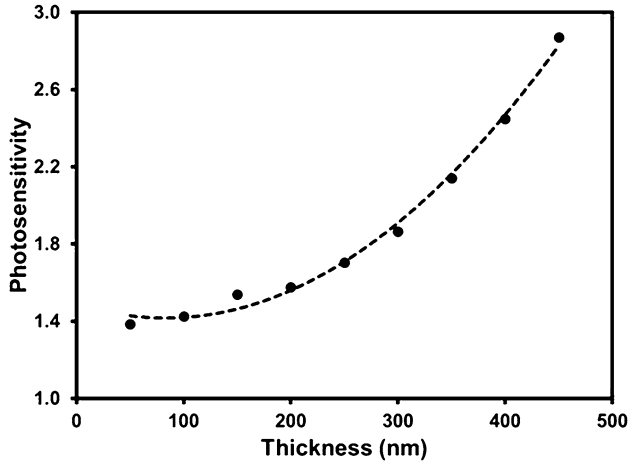

Fig. 8. The dependence of photosensitivity of nanocrystalline PbS films with thickness.

PbS films had an electrical conductivity of 10^{-4} S/cm at 300 K (RT). Nanocrystalline PbS films prepared by Kotadiya et al.[33] had electrical conductivity, mobility and hole concentration of 2.5×10^{-3} S/cm, 0.068 cm^{-2} V s and 2.2×10^{17} cm^{-1}, respectively; these films were also highly photoconducting.

The above results indicate that:

a. Simple direct coating of films from a precursor solution of lead acetate and thiourea in methanol produces nanocrystalline cubic PbS films.
b. The band gaps of the nanocrystalline PbS films are higher than that of bulk PbS (0.41 eV). The band gaps of nanocrystalline PbS films are thickness-tunable, as they progressively decrease from 2.4 eV to 1.6 eV as the thickness gradually increases from 50 nm to 450 nm.
c. The as-deposited nanocrystalline PbS films are *p*-type and photoconducting. The photoconductivity of these films increases monotonically with thickness.

Nanocrystalline PbS films with variable band gaps have been deposited by earlier workers[30–34] but only using CBD methods. In a typical CBD procedure, the substrates are kept in an aqueous bath of lead salt (acetate or nitrate), thiourea and a base (NaOH) for a deposition time of about 30–120 min. CBD with aqueous solution of lead acetate/lead nitrate, thiourea and NaOH generally yields polycrystalline PbS films.[39,40] Hence, to obtain nanocrystalline PbS films, Jana et al.,[30] Kaci et al.[31] and Pawar et al.[32] have added polyvinyl alcohol (PVA), polyethylene glycol (PEG 300) and trisodium citrate, respectively, to the bath. Alternatively, Kotadiya et al.[33] and Hussain et al.[34] used weak base NH_4OH (instead of NaOH) to prepare nanocrystalline PbS films. However, the CBD of PbS films is essentially cumbersome and time consuming. CBD also has the inherent disadvantage of being inefficient with low

material utilization factor and yield. In comparison, the process for direct coating of nanocrystalline PbS films is simple, faster and highly efficient with respect to material utilization. Further, the chemicals used for preparing precursor solution are minimal.

The tunability of band gap has been reported by earlier authors[30–32,34] but only for CBD nanocrystalline PbS films. Jana et al.[30] prepared nanocrystalline PbS films of thicknesses 650–700 nm with band gaps from 2.4 eV to 2.81 eV by varying the bath temperatures from 10°C to 30°C. Kaci et al.[31] found that band gaps of nanocrystalline PbS films can be varied from 0.9eV to 3.9 eV by varying the concentration of PEG from 0.2% to 1.5%. Pawar et al.[32] used deposition times (at 300 K) from 2 min to 90 min to produce nanocrystalline PbS films (thickness ~1–3 μm) with band gaps ranging from 1 eV to 2 eV. Hussain et al.[34] varied the concentration of lead acetate and thiourea from 0.05 M to 0.15 M to deposit nanocrystalline PbS films (thickness ~250 nm) with band gaps from 2.13 eV to 2.44 eV. The films of both Jana et al. and Hussain et al. showed tunability of the band gap in a narrow range of about 2.4 ± 0.4 eV with fixed and specific thicknesses only. The band gap tunability of PbS films prepared by Kaci et al. is quite wide (3 eV), but thicknesses are not mentioned. The band gap tunability of 1–2 eV for PbS films observed by Pawar et al. is for relatively thicker films (1–3 μm). In contrast, the nanocrystalline PbS films prepared by direct coating in the present study have band gap tunability in the range of 1.6–2.4 eV which varies gradually with thicknesses from 450 nm to 50 nm. This makes it easier to deposit PbS films with the desired band gaps as compared to CBD films.

The as-deposited PbS films are photoconducting and do not require special sensitization treatments such as oxidation in air[41] or inclusion of oxidants in the bath.[42] In the present investigation, the PbS films are made by heating LA-TU precursor films in air at 100°C. During the preparation process, oxygen is incorporated into the films which act as sensitization centres thus giving rise to photoconduction in the PbS films.

CONCLUSION

Band gap tunable PbS thin films can be deposited by direct coating from a precursor solution of lead acetate and thiourea in methanol. The process for deposition of PbS films is simple, at atmospheric pressure and at low temperatures. The films are smooth and shiny with a roughness (rms) of about 1.5 nm. The band gaps of the films gradually decrease from 2.4 eV to 1.6 eV as the thickness increases from 50 nm to 450 nm. The as-deposited films are photoconducting. The thickness tunability of the band gap makes these PbS films useful for technical applications, such as solar cells and photodetectors.

ACKNOWLEDGEMENT

The authors are grateful to the President and Provost of CHARUSAT for supporting this work. D.V. is grateful to the Department of Science and Technology (GoI) for providing an Inspire Fellowship.

REFERENCES

1. R. Debnath, J. Tang, D.A. Barkhouse, X. Wang, A.G. Pattantyus-Abraham, L. Brzozowski, L. Levina, and E.H. Sargent, *J. Am. Chem. Soc.* 132, 5952 (2010).
2. K. Szendrei, W. Gomulya, M. Yarema, W. Heiss, and M.A. Loi, *Appl. Phys. Lett.* 97, 203501 (2010).
3. J. Tang, L. Brzozowski, D.A.R. Barkhouse, X. Wang, R. Debnath, R. Wolowiec, E. Palmiano, L. Levina, A.G. Pattantyus-Abraham, D. Jamakosmanovic, and E.H. Sargent, *ACS Nano* 4, 869 (2010).
4. H. Choi, J. Kwan Kim, J. Hoon Song, Y. Kim, and S. Jeong, *Appl. Phys. Lett.* 102, 193902 (2013).
5. C. Piliego, L. Protesescu, S.Z. Bisri, M.V. Kovalenko, and M.A. Loi, *Energy Environ. Sci.* 6, 3054 (2013).
6. R. Debnath, M.T. Greiner, I.J. Kramer, A. Fischer, J. Tang, D.A.R. Barkhouse, X. Wang, L. Levina, Z.H. Lu, and E.H. Sargent, *Appl. Phys. Lett.* 97, 023109 (2010).
7. A.G. Pattantyus-Abraham, I.J. Kramer, A.R. Barkhouse, X. Wang, G. Konstantatos, R. Debnath, L. Levina, I. Raabe, M.K. Nazeeruddin, M. Grätzel, and E.H. Sargent, *ACS Nano* 4, 3374 (2010).
8. J. Tang, K.W. Kemp, S. Hoogland, K.S. Jeong, H. Liu, L. Levina, M. Furukawa, X. Wang, R. Debnath, D. Cha, K.W. Chou, A. Fischer, A. Amassian, J.B. Asbury, and E.H. Sargent, *Nat. Mater.* 10, 765 (2011).
9. I.J. Kramer and E.H. Sargent, *Chem. Rev.* 114, 863 (2014).
10. J.M. Luther, J. Gao, M.T. Lloyd, O.E. Semonin, M.C. Beard, and A.J. Nozik, *Adv. Mater.* 22, 3704 (2010).
11. P.R. Brown, R.R. Lunt, N. Zhao, T.P. Osedach, D.D. Wanger, L.Y. Chang, M.G. Bawendi, and V. Bulović, *Nano Lett.* 11, 2955 (2011).
12. J. Gao, C.L. Perkins, J.M. Luther, M.C. Hanna, H.Y. Chen, O.E. Semonin, A.J. Nozik, R.J. Ellingson, and M.C. Beard, *Nano Lett.* 11, 3263 (2011).
13. H. Wang, T. Kubo, J. Nakazaki, T. Kinoshita, and H. Segawa, *J. Phys. Chem. Lett.* 4, 2455 (2013).
14. C.-H.M. Chuang, P.R. Brown, V. Bulović, and M.G. Bawendi, *Nat. Mater.* 13, 1 (2014).
15. J. Tang, H. Liu, D. Zhitomirsky, S. Hoogland, X. Wang, M. Furukawa, L. Levina, and E.H. Sargent, *Nano Lett.* 12, 4889 (2012).
16. H. Liu, D. Zhitomirsky, S. Hoogland, J. Tang, I.J. Kramer, Z. Ning, and E.H. Sargent, *Appl. Phys. Lett.* 101, 1 (2012).
17. G. Konstantatos, I. Howard, A. Fischer, S. Hoogland, J. Clifford, E. Klem, L. Levina, and E.H. Sargent, *Nature* 442, 180 (2006).
18. G. Konstantatos and E.H. Sargent, *Appl. Phys. Lett.* 91, 173505 (2007).
19. G. Konstantatos, J. Clifford, L. Levina, and E.H. Sargent, *Nat. Photonics* 1, 531 (2007).
20. V. Sukhovatkin, S. Hinds, L. Brzozowski, and E.H. Sargent, *Science* 324, 1542 (2009).
21. C. Hu, A. Gassenq, Y. Justo, K. Devloo-Casier, H. Chen, C. Detavernier, Z. Hens, and G. Roelkens, *Appl. Phys. Lett.* 105, 171110 (2014).
22. J.P. Clifford, G. Konstantatos, K.W. Johnston, S. Hoogland, L. Levina, and E.H. Sargent, *Nat. Nanotechnol.* 4, 40 (2008).
23. B.N. Pal, I. Robel, A. Mohite, R. Laocharoensuk, D.J. Werder, and V.I. Klimov, *Adv. Funct. Mater.* 22, 1741 (2012).
24. F.W. Wise, *Acc. Chem. Res.* 33, 773 (2000).
25. L. Cademartiri, E. Montanari, G. Calestani, A. Migliori, A. Guagliardi, and G.A. Ozin, *J. Am. Chem. Soc.* 128, 10337 (2006).

26. I. Moreels, Y. Justo, B. De Geyter, K. Haustraete, J.C. Martins, and Z. Hens, *ACS Nano* 5, 2004 (2011).
27. M.A. Hines and G.D. Scholes, *Adv. Mater.* 15, 1844 (2003).
28. L. Cademartiri, J. Bertolotti, R. Sapienza, D.S. Wiersma, G. Von Freymann, and G.A. Ozin, *J. Phys. Chem. B* 110, 671 (2006).
29. I.J. Kramer, J.C. Minor, G. Moreno-Bautista, L. Rollny, P. Kanjanaboos, D. Kopilovic, S.M. Thon, G.H. Carey, K.W. Chou, D. Zhitomirsky, A. Amassian, and E.H. Sargent, *Adv. Mater.* 27, 116 (2015).
30. S. Jana, R. Thapa, R. Maity, and K.K. Chattopadhyay, *Phys. E Low-Dimens. Syst. Nanostruct.* 40, 3121 (2008).
31. S. Kaci, A. Keffous, M. Trari, H. Menari, and A. Manseri, *J. Alloys Compd.* 496, 628 (2010).
32. S.B. Pawar, J.S. Shaikh, R.S. Devan, Y.R. Ma, D. Haranath, P.N. Bhosale, and P.S. Patil, *Appl. Surf. Sci.* 258, 1869 (2011).
33. N.B. Kotadiya, A.J. Kothari, D. Tiwari, and T.K. Chaudhuri, *Appl. Phys. A Mater. Sci. Process.* 108, 819 (2012).
34. A. Hussain, A. Begum, and A. Rahman, *Indian J. Phys.* 86, 697 (2012).
35. T.K. Chaudhuri, H.N. Acharya, and B.B. Nayak, *Thin Solid Films* 83, L169 (1981).
36. P. Scherrer, *Nachr. Ges. Wiss. Göttingen* 2, 96 (1918).
37. J. Tauc and A. Menth, *J. Non. Cryst. Solids* 8–10, 569 (1972).
38. A.M. Fox, *Optical Properties of Solids*, 1st ed. (Oxford: Oxford University Press, 2001).
39. F. Kicinski, *Chem. Ind.* 17, 54 (1948).
40. S. Espevik, C. Wu, and R.H. Bube, *J. Appl. Phys.* 42, 3513 (1971).
41. R.H. Harada and H.T. Minden, *Phys. Rev.* 102, 1258 (1956).
42. G.H. Blount, P.J. Schreiber, D.K. Smith, and R.T. Yamada, *J. Appl. Phys.* 44, 978 (1973).